

## Supplementary material

### Enhancing the Lithium Storage Properties of Molten Salt-Etched $\text{Ti}_3\text{C}_2\text{T}_x$ through Sequential Intercalation of Alkali Ions

*Yanchao Ou,<sup>a</sup> Peng Zhang,<sup>\*a,b</sup> Razium Ali Soomro,<sup>a</sup> Ning Qiao,<sup>\*a</sup> Haonan Cui,<sup>a</sup> and Bin Xu<sup>\*a</sup>*

<sup>a</sup> State Key Laboratory of Organic-Inorganic Composites, Beijing Key Laboratory of Electrochemical Process and Technology for Materials, Beijing University of Chemical Technology, Beijing 100029, China. E-mail: zp7312769@163.com, qiaoning@mail.buct.edu.cn, binxumail@163.com

<sup>b</sup> Henan Key Laboratory of Photovoltaic Materials, School of Future Technology, Henan University, Zhengzhou 450046, China

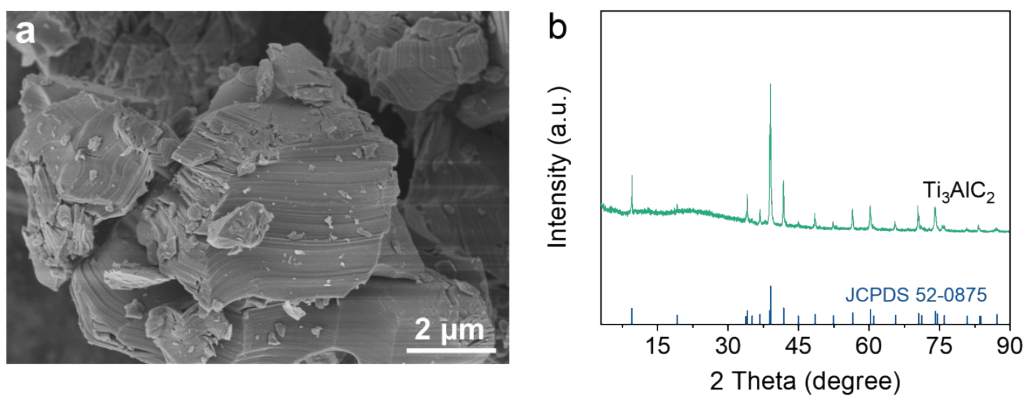


**Fig. S1** (a) SEM image and (b) XRD pattern of the  $\text{Ti}_3\text{AlC}_2$  powders.

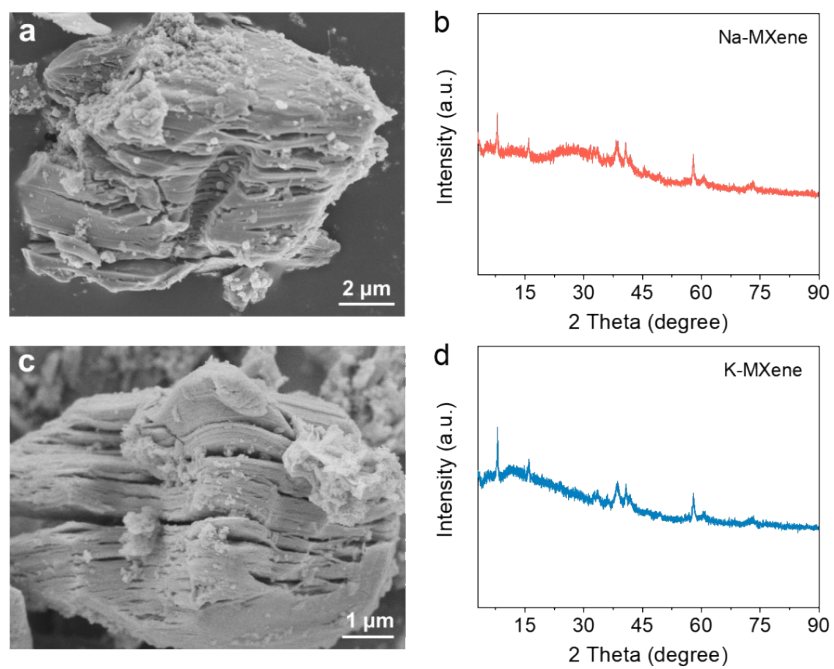


**Fig. S2** (a) SEM image and (b) XRD pattern of the Na-MXene, (c) SEM image and (d) XRD pattern of the K-MXene.

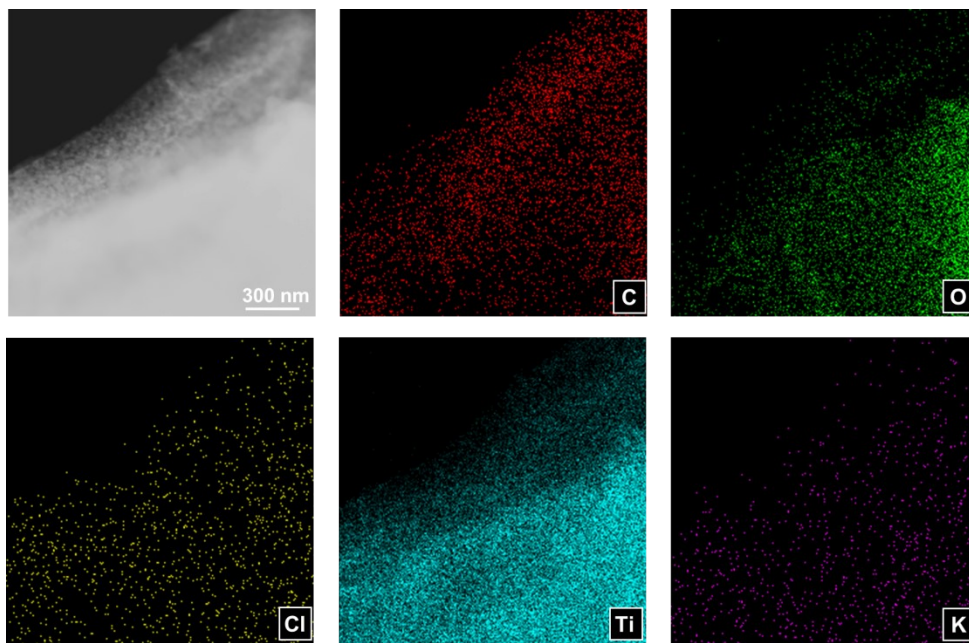


**Fig. S3** STEM images of K-MXene and corresponding elemental mappings showing distribution of C, O, Cl, Ti, and K elements.

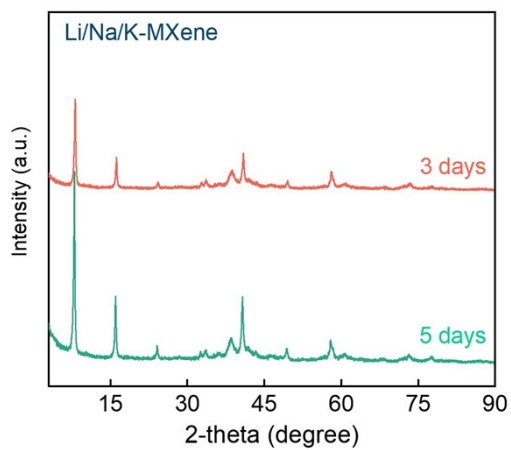


**Fig. S4** XRD patterns of the Li/Na/K-MXene post treating in the mixed alkaline solution after 3 and 5 days.

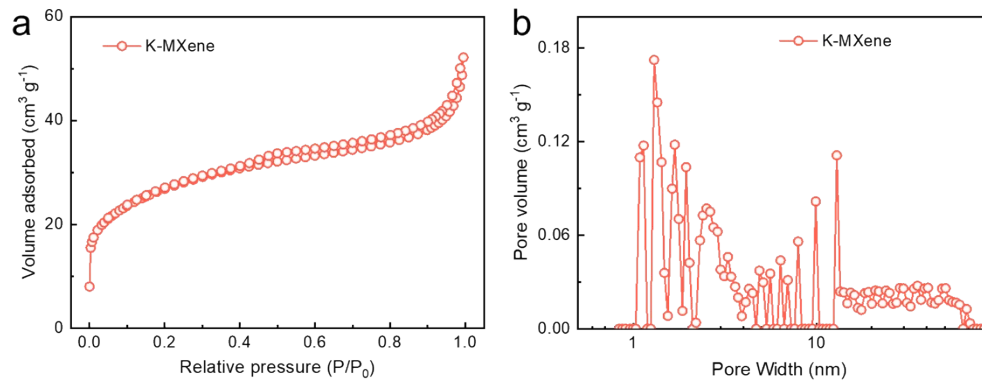


**Fig. S5** (a)  $N_2$  adsorption-desorption isotherm and (b) pore size distribution of the K-MXene.

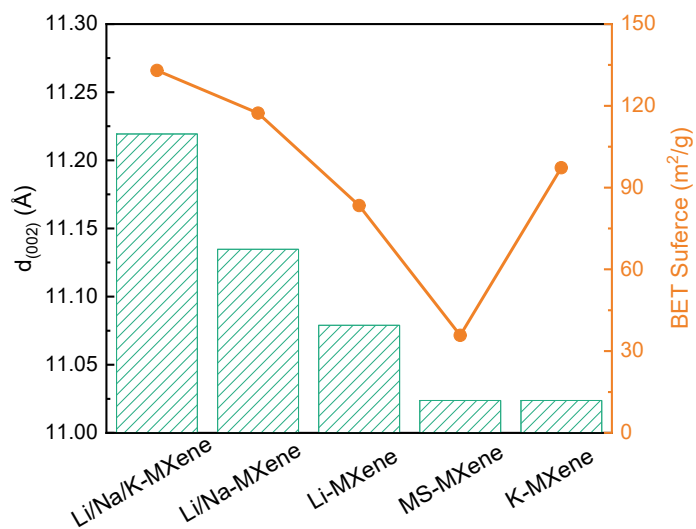


**Fig. S6** Relationship between interlayer spacings and specific surface areas of the AII-MXene in reference to MS-MXene.

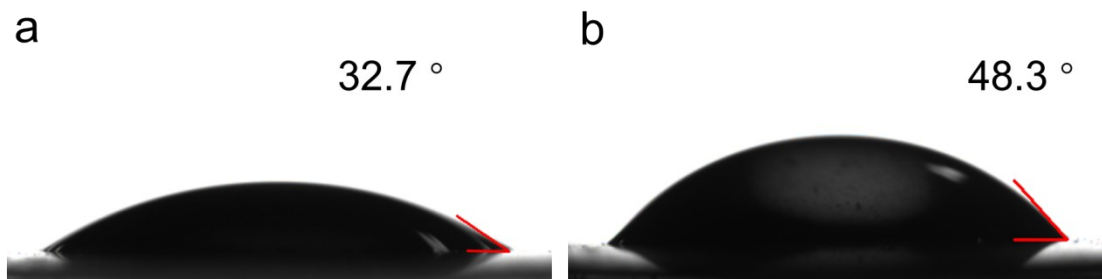


**Fig. S7** Water contact angles of the (a) Li/Na/K-MXene, and (b) MS-MXene.

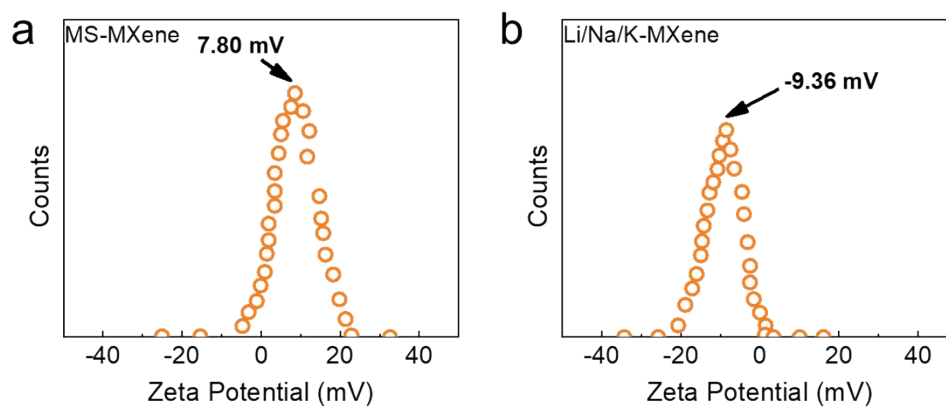


**Fig. S8** Zeta potentials of the (a) MS-MXene and (b) Li/Na/K-MXene.

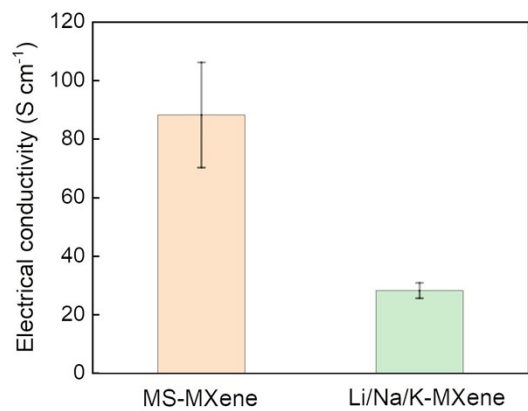


**Fig. S9** Electrical conductivities of the Li/Na/K-MXene and MS-MXene.

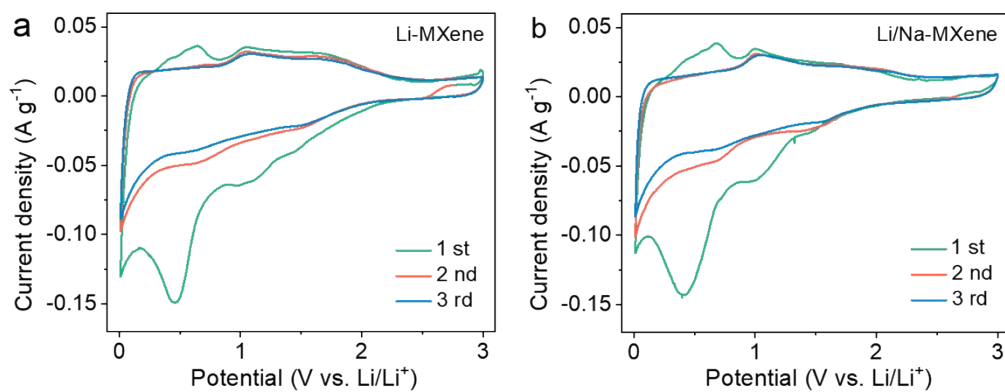


**Fig. S10** CV curves of the (a) Li-MXene and (b) Li/Na-MXene.

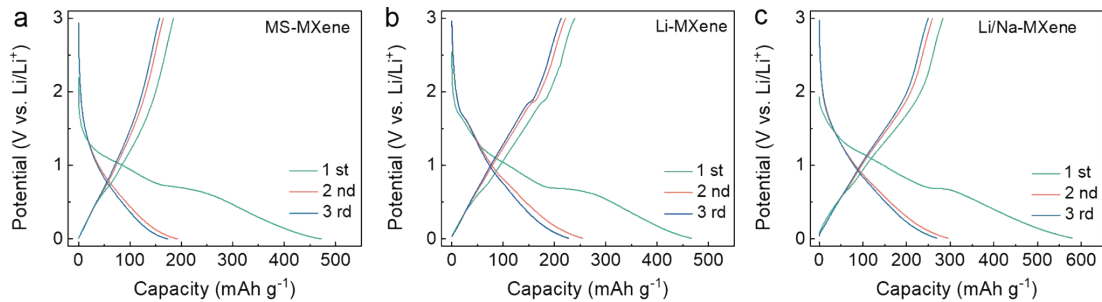


**Fig. S11** Galvanostatic charge/discharge curves of the (a) MS-MXene, (b) Li-MXene, and (c) Li/Na-MXene at a current density of 50 mA g<sup>-1</sup>.

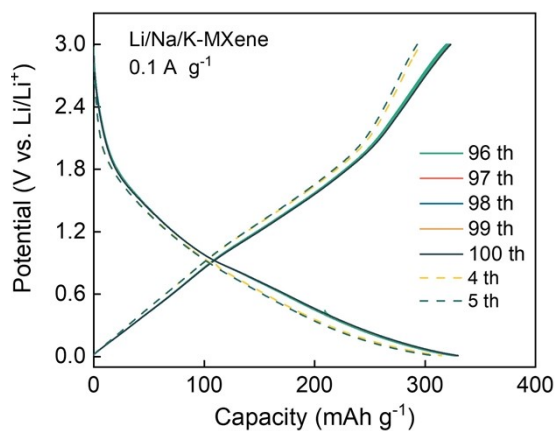


**Fig. S12** The last five GCD curves of the Li/Na/K-MXene during 100 cycles at 0.1 A g<sup>-1</sup>.

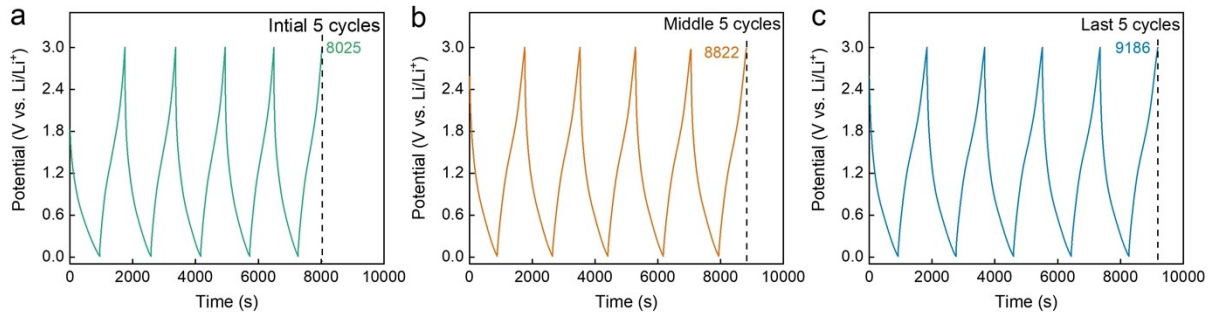


**Fig. S13** (a) initial, (b) middle, and (c) last five GCD curves of the Li/Na/K-MXene during 1200 cycles at 1 A g<sup>-1</sup>.

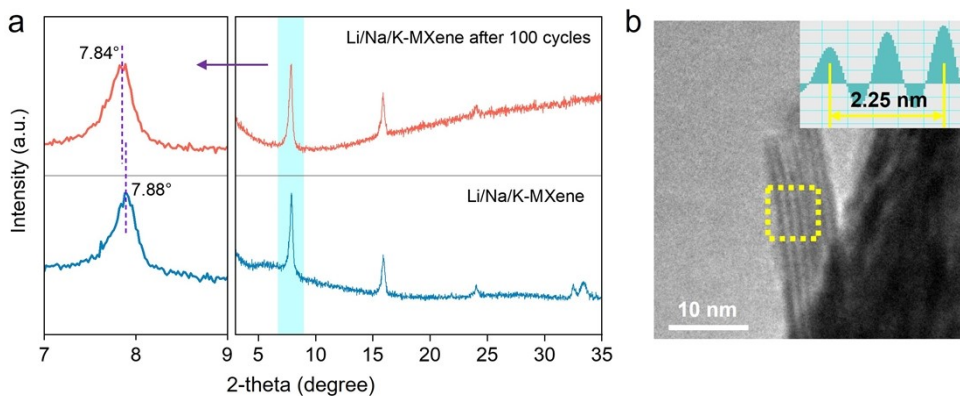


**Fig. S14** (a) XRD pattern and (b) TEM images of the Li/Na/K-MXene after 100 cycles at 1 A g<sup>-1</sup>.



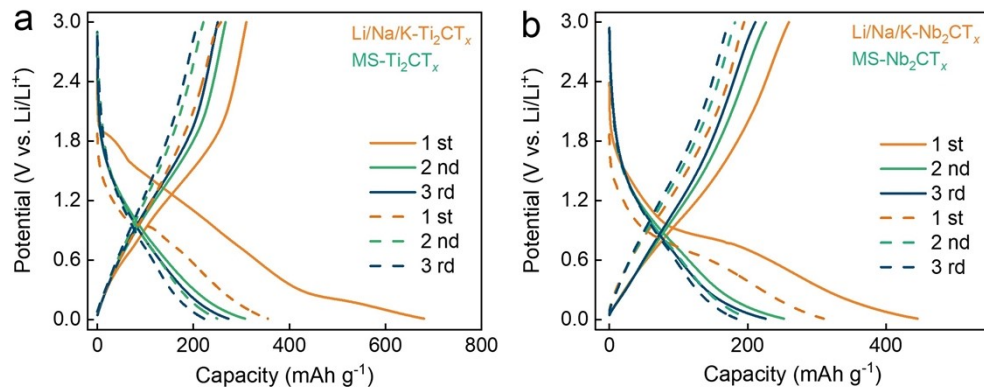


**Fig. S15** Initial three GCD curves at  $100 \text{ mA g}^{-1}$  of the (a)  $\text{Li/Na/K-Ti}_2\text{CT}_x$  and (b)  $\text{Li/Na/K-Nb}_2\text{CT}_x$  in comparison with their  $\text{MS-Ti}_2\text{CT}_x$  and  $\text{MS-Nb}_2\text{CT}_x$  counterparts.

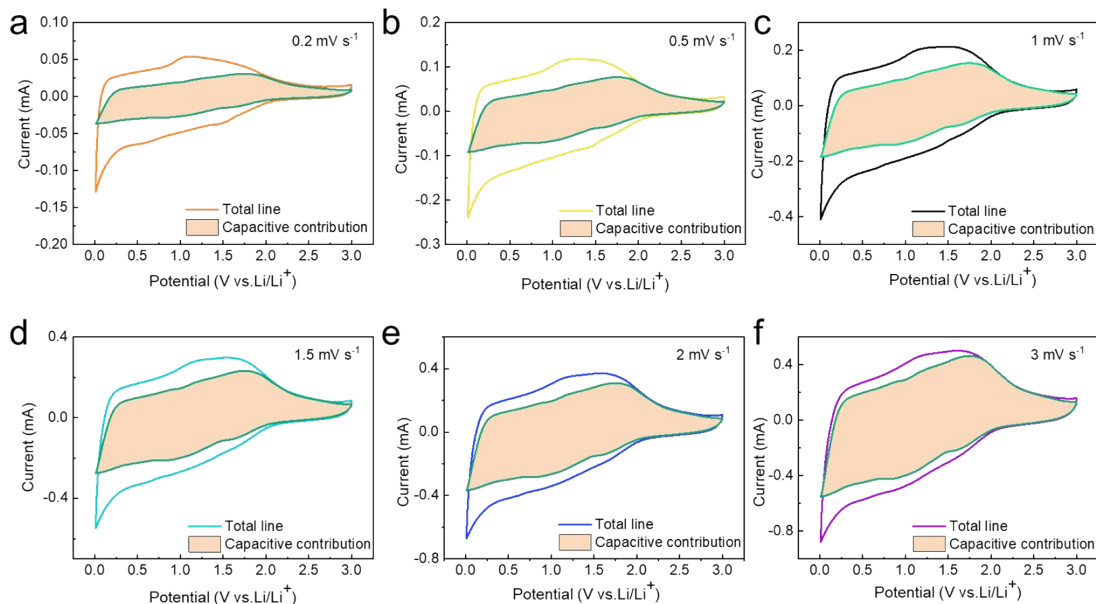


**Fig. S16** CV profile measured at various scan rates of (a) 0.2, (b) 0.5, (c) 1, (d) 1.5, (e) 2, and (f) 3  $\text{mV s}^{-1}$  with shaded area displaying the corresponding capacitive contributions for the  $\text{Li/Na/K-MXene}$ .

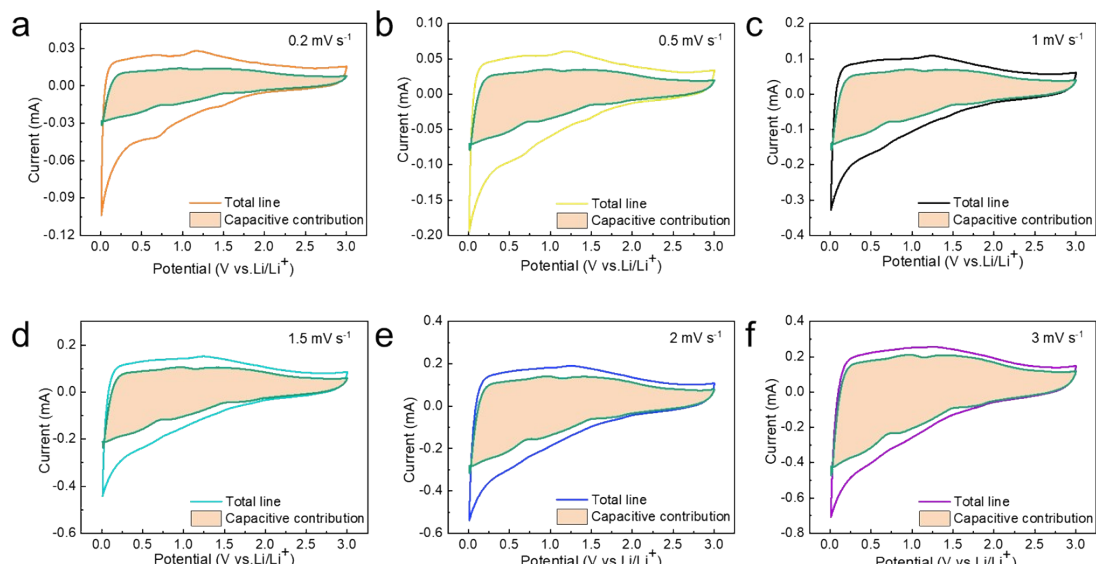


**Fig. S17** CV profile measured at various scan rates of (a) 0.2, (b) 0.5, (c) 1, (d) 1.5, (e) 2, and (f) 3  $\text{mV s}^{-1}$  with shaded area displaying the corresponding capacitive contributions for the MS-MXene.

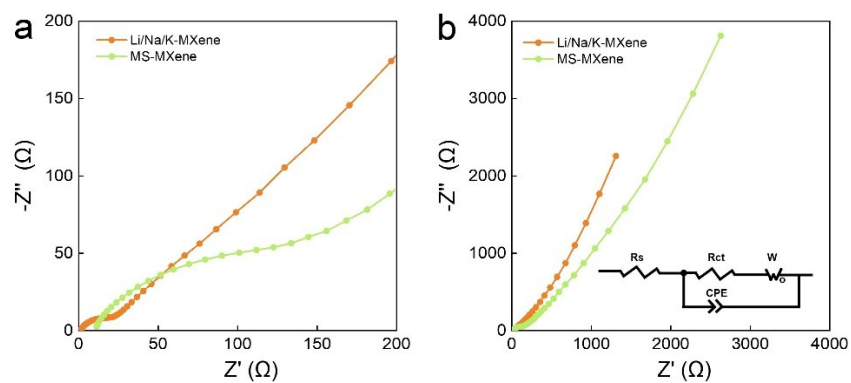


**Fig. S18** EIS spectra of the Li/Na/K-MXene and MS-MXene after 20 cycles at 50  $\text{mA g}^{-1}$ .

**Table S1** Comparison of the lithium storage properties of Li/Na/K-MXene with other previously reported MS-MXene.

Samples	Cycle performance			Rate performance		Ref.	
	Initial capacity (mAh g <sup>-1</sup> )	Current density (mA g <sup>-1</sup> )	Cycle number	Final capacity (mAh g <sup>-1</sup> )	Current density (A g <sup>-1</sup> )		Capacity (mAh g <sup>-1</sup> )
Li/Na/K-MXene	346.7	50	100	323.1	2	170.0	This work
		1000	1200	254.7			
Self-supported MS-MXene	225	200	-	-	2	~150	S1
	-	4000	2000	~85	16	95	
MS-Nb <sub>2</sub> CT <sub>x</sub>	305	100	-	-	2	~150	S2
	-	1000	1500	~190	10	80	
MS-Ti <sub>3</sub> C <sub>2</sub> T <sub>x</sub>	-	-	-	-	~0.12 (0.6 C)	205	S3
	-	-	-	-	~1.8 (13 C)	142	
Cl-terminated Ti <sub>2</sub> CT <sub>x</sub>	-	-	-	-	0.1	277	S4
	-	-	-	-	2	162	
Ti <sub>3</sub> C <sub>2</sub> Br <sub>x</sub>	-	-	-	-	0.05	189	S5
	-	1000	1000	~80	2	70	
MS-Ti <sub>2</sub> CT <sub>x</sub>	-	500	200	99.2	2	88.0	S6
	-				8	57.6	

## References

- [S1] L. Liu, M. Orbay, S. Luo, S. Duluard, H. Shao, J. Harmel, P. Rozier, P-L. Taberna, P. Simon, Exfoliation and Delamination of  $Ti_3C_2T_x$  MXene Prepared via Molten Salt Etching Route. *ACS Nano*, **2022**, 16, 111-118.
- [S2] H. Dong, P. Xiao, N. Jin, B. Wang, Y. Liu, Z. Lin, Molten Salt Derived  $Nb_2CT_x$  MXene Anode for Li-ion Batteries. *ChemElectroChem.*, **2021**, 8, 957-962.
- [S3] Y. Li, H. Shao, Z. Lin, J. Lu, L. Liu, B. Duployer, P. O. Å. Persson, P. Eklund, L. Hultman, M. Li, K. Chen, X. -H. Zha, S. Du, P. Rozier, Z. Chai, E. Raymundo-Piñero, P.-L. Taberna, P. Simon, Q. Huang, A General Lewis Acidic Etching Route for Preparing MXenes with Enhanced Electrochemical Performance in Non-Aqueous Electrolyte. *Nat. Mater.*, **2020**, 19, 894-899.
- [S4] G. Ma, H. Shao, J. Xu, Y. Liu, Q. Huang, P-L. Taberna, P. Simon, Z. Lin, Li-Ion Storage Properties of Two-Dimensional Titanium-Carbide Synthesized via Fast One-Pot Method in Air Atmosphere. *Nat. Commun.*, **2021**, 12, 5085.
- [S5] P. Liu, P. Xiao, M. Lu, H. Wang, N. Jin, Z. Lin, Lithium Storage Properties of  $Ti_3C_2T_x$  ( $T_x = F, Cl, Br$ ) MXenes. *Chin. Chem. Lett.*, **2023**, 34, 107426.
- [S6] P. Huang, H. Ying, S. Zhang, Z. Zhang, W-Q. Han, In situ Fabrication of MXene/CuS Hybrids with Interfacial Covalent Bonding via Lewis Acidic Etching Route for Efficient Sodium Storage. *J. Mater. Chem. A*, **2022**, 10, 22135-22144.